Proceedings of DETC'03
ASME 2003 Design Engineering Technical Conferences and
Computers and Information in Engineering Conference
Chicago, Illinois, USA, September 2-6, 2003

DETC2003/VIB-48525

HYSTERESIS EFFECT IN ADHESIVE ELASTIC CONTACT

Zheng Wei, Ya-Pu Zhao
State Key Laboratory of Non-linear Mechanics, Institute of Mechanics,
Chinese Academy of Sciences, Beijing 100080, China
E-mail yzhao@lnm.imech.ac.cn, Tel: 86-10-62658008

ABSTRACT

Adhesive forces in microscale or nanoscale contact play a significant role in microelectromechanical systems (MEMS); scanning probe microscope (SPM) and some other related fields. In this paper, the relationship between the pull-off force and the transition parameter as well as the variation of the pull-off radius with the transition parameter is given. When hysteresis effect is considered, hysteresis models are presented to describe the contact radius as a function of external load in loading and unloading processes. Among these models, we verified the hysteresis model from JKR, which is in a good agreement with experiment. The parameter α of dissipated elastic energy can be measured through experiment.

1. INTRODUCTION

Adhesion is one of the major factors that limit the widespread use of microelectromechanical systems (MEMS), so it attracts much attention in the MEMS community [1]. In nanoscale level, adhesion between the tip of the atomic force microscope (AFM) and a surface is capital for understanding the imaging mechanism. Continuum mechanics models of the adhesion between two spherical surfaces that deform within the elastic limit are well developed. Bradley [2] calculated the force to separate two rigid spheres in 1932. Adhesive contact theories of deformable spheres were presented by Johnson, Kendall and Roberts [3] in 1971 (JKR theory) and by Derjaguin, Muller and Toporov [4] in 1975 (DMT theory), and these two theories led to a rather acrimonious debate. The situation was resolved by Tabor [5], who suggested that the two models were each appropriate to opposite extremes of a dimensionless parameter μ (Tabor number). This parameter may be interpreted as a measure of the magnitude of the elastic deformation compared with the range of surface forces. Thus, large values of μ correspond to soft materials with large surface energy and radius (JKR model) and small values to hard solids of small radius and low surface energy (DMT model). In 1992, Maugis [6](M-D), using the Dugdale model, provided an analytical solution to it. In this model, a transition parameter λ ($\lambda = 1.16\mu$) is introduced. When λ increases from zero to infinity, there is a continuous transition from DMT to JKR models. To our knowledge, apart from some authors gave the relationship between the pull-off force and the transition parameter [7], the variation of the pull-off radius with the transition parameter is still lacking so far.

For elastic materials, the contact radius is determined by the applied load, the elastic properties of the contacting materials, and the work of adhesion [8]. Most real processes involving adhesion are hysteretic even though they usually described in terms of (ideally) reversible thermodynamic functions. The work done on separating two surfaces from adhesive contact is generally not fully recoverable by bringing the two surfaces back into contact again. This may be referred to as adhesion hysteresis [9]. Understanding hysteresis behavior will be critical in developing technologies to control adhesion. Dutroski [10] first observed hysteresis in contact deformation. Frantz et al. [11] used a capacitive method to obtain the surface forces and the hysteresis loop. An atomic force microscope (AFM) can also be used to measure the hysteresis between a tip attached to the cantilever and the surface of a sample [12-14]. Many evidences indicate that hysteresis observed at the interface between elastic solids is the result of nonequilibrium processes occurring at the interface, such as physicochemical reconstruction, increase of surface roughness due to extraction, elastic instabilities, and viscoelastic bulk deformations when the contacting materials are not perfectly elastic [15-18]. Assuming that a fraction α of the elastic energy is dissipated, Johnson obtained the relationship between the energy release rate and the work of adhesion [19]. The energy release rate has been studied in details by Maugis [6]. This paper applies the theories of Johnson and Maugis to derive the relationship between the external load and the contact radius. Some revised

models from JKR, DMT and M-D are presented. Moreover, an experiment is compared to the hysteresis model from JKR.

2. CONTINUUM MODELS OF ADHESIVE CONTACT

2.1 Bradely theory

When two rigid spheres are in contact, the attractive force is described as [2]

$$F_0 = 2\pi R w_a , \tag{1}$$

where $R = R_1 R_2 /(R_1 + R_2)$ is the equivalent radius, R_1 and R_2 are the radii of the two spheres respectively, and w_a is the Dupré energy of adhesion or work of adhesion [20]:

$$w_a = \gamma_1 + \gamma_2 - \gamma_{12} , \tag{2}$$

where γ_1 and γ_2 are the surface energies of the two solid surfaces, respectively, and γ_{12} is the interfacial energy.

2.2 DMT theory

Considering the two spheres are deformable, Derjaguin, Muller and Toporov gave the amendatory Hertzian model [4]

$$\frac{a^3 K}{R} = p + 2\pi R w_a , \tag{3}$$

where $K = \frac{4}{3}\left[(1-\upsilon_1^{\,2})/E_1 + (1-\upsilon_2^{\,2})/E_2\right]^{-1}$, υ is the Poisson ratio and E is the Young's modulus, and the suffixes refer to the two spheres, p is the external force, and a is the contact radius resulted from the external force and the adhesive forces.

2.3 JKR theory

Johnson et al. presented their model for two contacting spheres [3]. Similar to DMT model, the contact area in JKR theory is larger than that in Hertz theory. The relationship between the contact radius and the forces (both the external load and adhesive force) is shown as [3]

$$\frac{a^3 K}{R} = p + 3\pi R w_a + \sqrt{6\pi w_a R p + (3\pi w_a R)^2} . \tag{4}$$

2.4 M-D theory

Maugis used the Dugdale approximation to estimate the value of the contact radius, referred as M-D solution [21]. The contact radius and the external force are related by

$$\frac{1}{2}\lambda \bar{a}^{-2}\left[(m^2-2)\arccos(1/m) + \sqrt{m^2-1}\right] + \frac{4}{3}\lambda^2 \bar{a}^{-1}\left[\sqrt{m^2-1}\arccos(1/m) - m + 1\right] = 1 , \tag{5}$$

$$\bar{p} = \bar{a}^3 - \lambda \bar{a}^2\left[\sqrt{m^2-1} + m^2\arccos(1/m)\right], \tag{6}$$

where $\bar{p}$ and $\bar{a}$ are simple parameterizations of p and a, $\bar{p} = p/\pi w_a R$ □ $\bar{a} = \left(\frac{4E^*}{3\pi w_a R^2}\right)^{1/3} a$, λ is the transition parameter, $\lambda = 1.16\mu$, μ is Tabor number as $\mu = \left(\frac{R w_a^{\,2}}{E^{*2}\varepsilon^3}\right)^{1/3}$, where ε is the equilibrium space between atoms, and the parameter m represents the ratio of the contact radius a to the outer radius described in Dugdale model. The difficulty in utilizing the M-D equations lies in the lack of a direct expression relating a to p.

3. PULL-OFF FORCE AND PULL-OFF RADIUS

As previously discussed, there exists an adhesive force in the contact area. An atomic force microscope is a good example to interpret the pull-off force and pull-off radius. A typical force-distance curve obtained by AFM is depicted in Fig.1. The force between the AFM tip and the surface is quantified along the vertical axis, while the horizontal axis shows the surface displacement coordinate. As an AFM tip approaches the surface, initially there is no detectable interaction, when the tip is close enough to the surface, the tip "jumps in" to the surface, the tip is further pushed into the surface and their interaction becomes repulsive. When the tip is withdrawn, the repulsive force is replaced by attractive force. When the cantilever's spring force is great enough to overcome the adhesive force, the cantilever tip jumps back to its original position. This is called a "pull-off" event, and at the same time, the adhesive force is defined as "pull-off force", the contact radius is named "pull-off radius". This phenomenon exists in many contact processes.

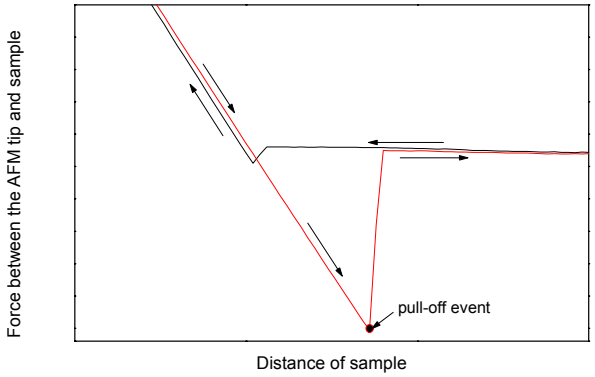

Fig.1. Force–distance curves for approach and retraction using a Dimension 3000 AFM in ambient conditions. The scan rate (loading/unloading rate) was 0.2 Hz. The curves show a significant hysteresis phenomenon.

For DMT model, according to Eq. (3), the pull-off force p is $2\pi R w_a$, and the contact radius is zero. In JKR model, the pull-off force can be derived from Eq. (4). The minimum load p meets

$$p_{pull-off} = \frac{3}{2}\pi w_a R , \tag{7}$$

and then the pull-off radius can be obtained easily. There are some differences between JKR model and DMT model. When Tabor introduced a dimensionless number (Tabor number), the contradiction was resolved [5]. Although Johnson et al. [7] has

discussed the transition between JKR and DMT theories by the transition parameter λ (λ equals to 1.16 times of Tabor number), the variation of pull-off radius with transition parameter λ is not included. It is rather cumbersome to carry out the pull-off force and the pull-off radius for M-D model. When λ is fixed, there exists a conditional extremum under the restriction of Eq. (6). The value of p can be determined by numerical methods, and the pull-off radius can be obtained subsequently.

The pull-off force and pull-off radius can be presented in the transition parameter, and the related curves can be drawn. Fig.2 shows the relationship between the pull-off force versus the transition parameter λ, and Fig.3 gives the curve of the pull-off radius versus the parameter. In order to compare M-D model to the other models, DMT and JKR models are also shown in the figures. The Fig.3 also shows that with the increase of the transition parameter λ, values of both the pull-off force and the pull-off radius vary continuously from DMT model to JKR model. It is consistent with Fig.2.

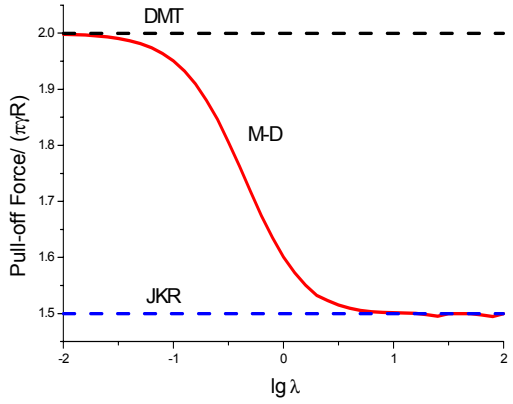

Fig.2. Pull-off force versus λ determined from the M-D, DMT and JKR models [7].

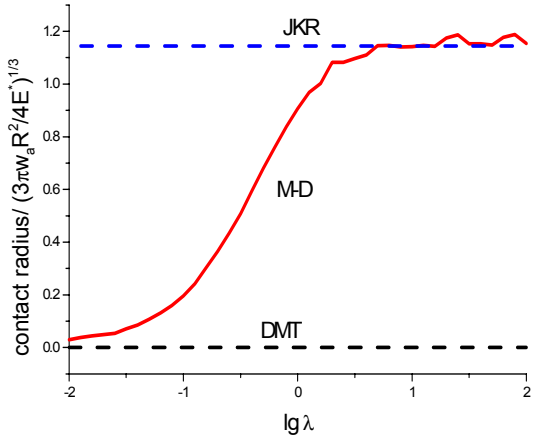

Fig.3. Pull-off radius versus λ from M-D, DMT and JKR models.

4. HYSTERESIS EFFECT

Experimentally, adhesion hysteresis is defined as the difference between loading and unloading process. This type of hysteretic behavior is common with most practical interfacial phenomena, such as wetting. Fig.1 shows a typical hysteresis between an AFM tip and the surface of a sample. During the retracting process, a clear force hysteresis occurs due to the attractive force and bond formation between the tip and surface. More work must be done to separate the tip from the substrate.

In practical adhesion systems, hysteresis occurs by the combination of many effects, which are usually highly coupled. Therefore, for the fundamental research on hysteresis, it is desirable to use simple model that can provide fundamental mechanism. In this work, the authors assumed that a fraction of energy must be dissipated in the approaching and receding processes. Here the model was named hysteresis model. Maugis et al. [22] regarded the edge of the contact area as a crack that recedes or advances when the contact area increases or decreases. In 1968, Rice introduced the J-integral to compute the energy release rate G from the stresses on the path surrounding the cohesive zone. The elastic energy release rate is equal to the work done against surface forces,

$$G = w_a . \tag{8}$$

If a fraction α of the elastic energy is dissipated, the released energy has to overcome the dissipation and the work of adhesion during separation, i.e. [19]

$$G = w_a + \alpha G . \tag{9}$$

During approach process, G and w_a change sign, but the dissipation does not, i.e. [19]

$$-G = -w_a + \alpha G . \tag{10}$$

In theoretically, the fraction α is something coupled with materials' properties, contacting geometrical shape, loading-unloading rates and so on. It is still a complicated parameter at all. However, from phenomenon, and for a matter, the fraction α can be obtained from experiments.

Based on the assumption as just discussed, we can revise models in the second section. More reasoned discuss is in the following section.

4.1 Hysteresis model from JKR

In JKR model, the energy release rate is given as [6]

$$G = \frac{(p_1 - p)^2}{6\pi a^3 K} = \frac{3K}{8\pi a}\left(\delta - \frac{a^2}{R}\right)^2 , \tag{11}$$

where $p_1 = \frac{3aK}{2}\left[\int_0^1 \frac{f'(x)dx}{\sqrt{1-x^2}} - \int_0^1 \frac{xf(x)dx}{\sqrt{1-x^2}}\right]$. When a sphere is contacting with a plane, $f(x) = \frac{a^2}{R^2}x^2, x = \frac{r}{a}$.

Substituting these to the expression of p_1, $p_1 = \frac{a^3 K}{R}$. The Griffith criterion gives the equilibrium relation:

$$G = \frac{\left(p - \frac{a^3 K}{R}\right)^2}{6\pi a^3 K} = w_a . \qquad (12)$$

In fact, Eqs. (12) and (4) are equivalent. When the loss of energy is considered, the equilibrium equation in hysteresis model should be rewritten. Substituting Eq. (12) into Eqs. (9), (10) gives

$$\frac{\left(p - \frac{a^3 K}{R}\right)^2}{6\pi a^3 K} = \frac{w_a}{1+\alpha}, \text{ or}$$

$$\frac{a^3 K}{R} = p + 3\pi R \frac{w_a}{1+\alpha} + \sqrt{6\pi R p w_a /(1+\alpha) + (3\pi w_a R/(1+\alpha))^2}$$

(in loading case), (13)

$$\frac{\left(p - \frac{a^3 K}{R}\right)^2}{6\pi a^3 K} = \frac{w_a}{1-\alpha}, \text{ or}$$

$$\frac{a^3 K}{R} = p + 3\pi R \frac{w_a}{1-\alpha} + \sqrt{6\pi R p w_a /(1-\alpha) + (3\pi w_a R/(1-\alpha))^2}$$

(in unloading case). (14)

Eq. (14) shows that the pull-off force and the pull-off radius are both larger than those in JKR model.

It is well known that hysteresis is a key problem in understanding physical phenomena of adhesion. From the models we have just established, the loop of loading and unloading processes for hysteresis model from JKR versus JKR model is shown in Fig.4. The curves of loading and unloading processes are illustrated in Fig.5, in which the load and the contact radius have been normalized as: $\bar{p} = \frac{p}{\pi R w_a}$, $\bar{a} = \frac{a}{a_0}$, a_0 is the contact radius at the zero load in JKR model, and the dissipated fraction $\alpha = 0, 0.25, 0.5, 0.75$. It is clear from Fig.5 that when the dissipated fraction $\alpha \to 0$, the hysteresis model from JKR tends towards JKR, and when the dissipated fraction α is increased, either the pull-off force or the pull-off radius is increased.

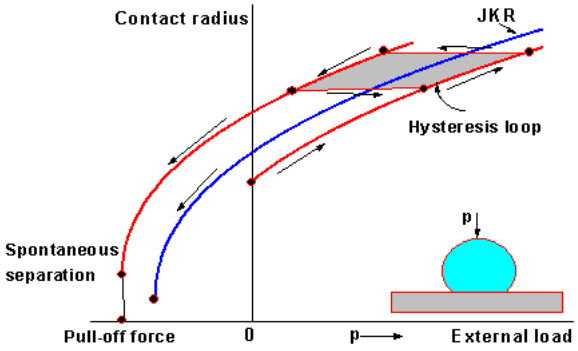

Fig.4. Hysteresis loop and JKR plot. When dissipated energy is considered, and before the separation is come, a close loop will be formed during transformation between loading and unloading. The JKR plot is between the loading and unloading curves as the hysteresis effect is taken into account

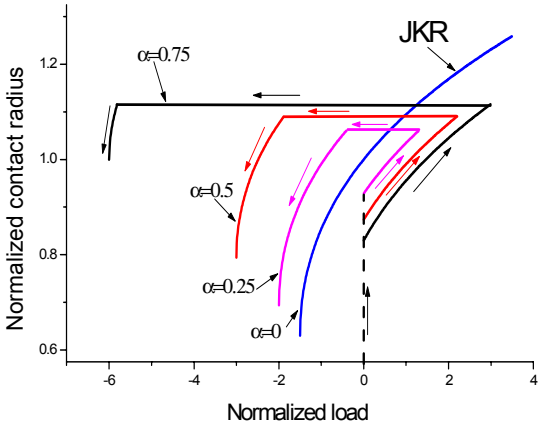

Fig.5. Adhesion hysteresis. Loading and unloading curves using hysteresis model from JKR with different fraction α. The results show that with the fraction α is greater, the loading path is further from the unloading path.

4.2 Hysteresis model from DMT

According to Eq. (3), the energy release rate can be determined as:

$$G = \left(\frac{a^3 K}{R} - p\right) / 2\pi R \qquad (15)$$

Similarly, for hysteresis model, the relationship between external load and contact radius during loading and unloading is

$$\frac{a^3 K}{R} = p + 2\pi R w_a /(1+\alpha), \qquad (16)$$

$$\frac{a^3 K}{R} = p + 2\pi R w_a /(1-\alpha). \qquad (17)$$

Eq. (17) also shows that the pull-off force in hysteresis model is larger than that in DMT model, but the pull-off radius is zero as that in DMT.

4.3 Hysteresis model from M-D

The expression of the energy release rate for M-D model is [6]

$$G = \frac{p_1 - p}{2\pi R}\left(1 - \frac{2arctg\sqrt{m^2-1}}{\sqrt{m^2-1} + m^2 arctg\sqrt{m^2-1}}\right) + \frac{4(1-\upsilon^2)}{E} K_I^{\,2} \frac{\sqrt{m^2-1}\,arctg\sqrt{m^2-1} - m + 1}{\left(\sqrt{m^2-1} + m^2 arctg\sqrt{m^2-1}\right)^2}, \quad (18)$$

where $K_I = \frac{p_1 - p}{2\pi R}$. When $m \to 1$, one can get the result of JKR, and when $m \to \infty$, the result is DMT. It is easy to obtain loading and unloading equilibrium equations from Eqs. (18), (9) and (10).

4.4 Discussion and comparison to experiment

By comparison, the pull-off forces in our hysteresis models are larger than those determined by corresponding JKR and DMT models. The pull-off radius given by hysteresis model is larger than that in JKR, but equal to that in DMT. Because the loading and unloading curves are not the same path, extra work is required to separate the contact surfaces. When the contact process is switched from loading to unloading, the contact radius holds unchanged until the load decrease to a defined value that meets the energy release rate of unloading process in Eq. (14). In general, we attribute hysteresis to complex phenomena occurring at the interface, namely impact contact, viscoelastic or plastic bulk deformation of the contact materials, surface roughness, reorientation, interdiffusion, and interdigitation of the molecules. These processes have a common property that is energy dissipated, so a fraction α is introduced to characterize these processes.

In the discussion of hysteresis, the whole process is described clearly by a parameter α. In practice, as a result of the complication of hysteresis, more studies must be undertaken for all of the factors that result in adhesion hysteresis. Fig.6 shows compression/decompression cycles of mica sheets covered with laterally ordered DCDDBr monolayers while varying the relative humid [23]. The experiment approves our model from JKR. On unloading, the contact area does not initially fall, or it falls much less rapidly than expected from the JKR equation. Based on our model from JKR, the fraction α can be obtained from parameter fitting. The estimated results are $\alpha = 0.32$ for the first part of Fig.6. and $\alpha = 0.08$ for the second part. It should be noted that our models is simplified, they couldn't be agree with all experiments at any cases, for the fraction α may be variable in the process from loading to unloading.

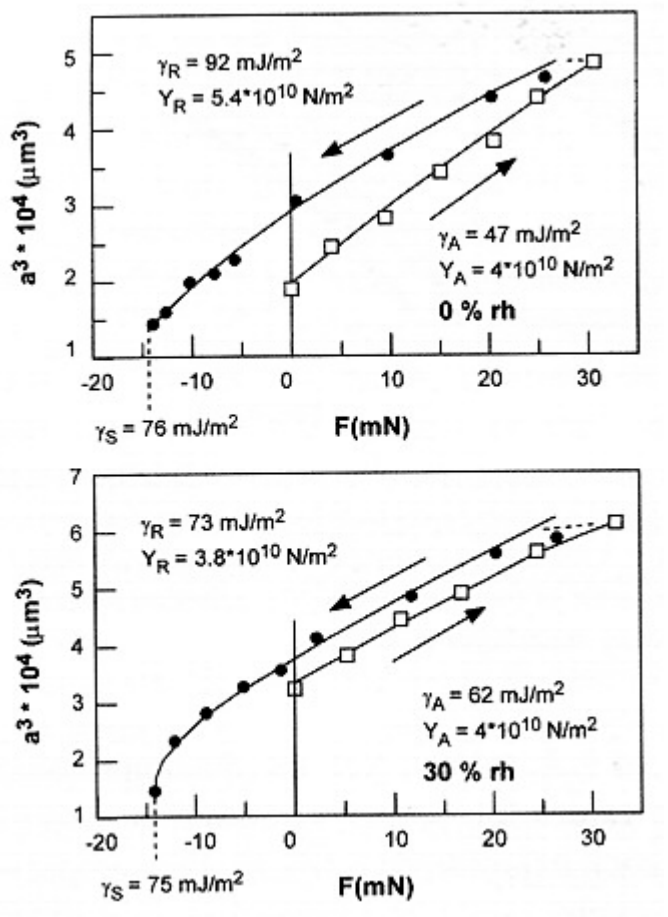

Fig.6. Compression/decompression cycles of mica sheets covered with laterally ordered DCDDBr monolayers while varying the relative humid [23].

5. CONCLUSIONS

DMT model and JKR model are the extreme cases of M-D model. Some authors draw this conclusion through the relation between pull-off force and transition parameter λ. We verify the conclusion through the relation between the pull-off radius and transition parameter λ. When the transition parameter λ tends to be very small (i.e., stiff materials, weak adhesion forces, small tip radii), DMT theory is identical to M-D theory. On the contrary, when λ becomes very large (i.e., compliant materials, strong adhesion forces, large tip radii), M-D theory reduces to JKR theory.

Adhesive contact hysteresis is a complicated process, which is contributed to many factors, but there is common property in this process. That is energy dissipated. Some revised models are presented to characterize the complicated loading and unloading processes on such fact. Among these models, the hysteresis model from JKR is in good agreement with the experimental results.

ACKNOWLEDGMENTS

The project is supported by the Distinguished Young Scholar Fund of NSFC (Grant No. 10225209), key project from the Chinese Academy of Sciences (Grant No. KJCX2-SW-L2) and National "973" Project (No. G1999033103).

Discussions with Professor Christiane Helm are gratefully appreciated. Also, she supplied the legible image of Fig.6 of this paper.

REFERENCES

[1] Zhao Y P, Wang L S and Yu T X 2003 *J. Adhesion Sci. Technol.*, **17** 519
[2] Bradley R S 1932 *Phil. Mag*. **13** 853
[3] Johnson K L, Kendall K and Roberts A D 1971 *Proc. R. Soc. London A* **324** 301
[4] Derjaguin B V, Muller V M and Toporov Y P 1975 *J. Colloid Interface Sci*. **53** 314
[5] Tabor D 1976 *J. Colloid Interface Sci.* **58** 1
[6] Maugis D 1992 *J. Colloid interface Sci.* **50** 243
[7] Johnson K L and Greenwood J A 1997 *J. Colloid Interface Sci.* **192** 326
[8] Zhao Y P 2003 *Acta Mechanica Sinica* **19** 1
[9] Israelachvili J N 1992 *Fundamentals of friction: Macroscopic and Microscopic Processes,* (Singer I L and Pollock H Mkluwer eds. Netherlands: Academic Publishers)
[10] Dutroski R C 1969 *Trans. ASME, J.Lubr Technol.* **91F** 732
[11] Frantz P, Artsyukhovich A, Carpick R W and Salmeron M 1997 *Langmuir* **13** 5957
[12] Jacquot C and Takadoum J 2001 *J. Adhesion Sci. Technol.* **15** 681
[13] Segeren L, Siebum B, Karssenberg F, Berg J and Vancso G 2002 *J. Adhesion Sci. Technol*. **16** 793
[14] Méndez-Vilas A, González-Martín M, Labajos-Broncano L and Nuevo M 2002 *J. Adhesion Sci. Technol.* **16** 1737
[15] Chaudhury M K and Whitesides G M 1991 *Langmuir* **7** 1013
[16] Chen Y L, Helm C A and Israelachvili J N 1991 *J. Phys. Chem*. **95** 10737
[17] Attard P and Paker J L 1992 *Phys. Rev. A* **46** 7959
[18] Scmitt F J, Yoshizawa H, Schmidt A, Duda G, Knoll W, Wegner G and Israelachvili J N 1995 *Macromolecules* **28** 3401
[19] Johnson K L 1998 *Tribology Int*. **31** 413
[20] Israelachvili J N 1985 *Intermolecular and Surface Forces,* (Florida: Academic Press Inc)
[21] Johnson K L 1997 *Proc. R. Soc. London A* **453** 163
[22] Maugis D, Barquins M and Courtel R 1976 *Mét. Corro Indu* **No.605** 1
[23] Mächtle P and Helm C A 1998 *Thin Solid Films* **330** 1